

# An Amide-Containing Metal–Organic Tetrahedron Responding to a Spin-Trapping Reaction in a Fluorescent Enhancement Manner for Biological Imaging of NO in Living Cells

Jian Wang, Cheng He,\* Pengyan Wu, Jing Wang, and Chunying Duan\*

State Key Laboratory of Fine Chemicals, Dalian University of Technology, Dalian, 116012, China

**S** Supporting Information

**ABSTRACT:** Metal–organic polyhedra represent a unique class of functional molecular containers that display interesting molecular recognition properties and fascinating reactivity reminiscent of the natural enzymes. By incorporating a triphenylamine moiety as a bright blue emitter, a robust cerium-based tetrahedron was developed as a luminescent detector of nitronyl nitroxide (PTIO), a specific spin-labeling nitric oxide (NO) trapper. The tetrahedron encapsulates molecules of NO and PTIO within the cavity to prompt the spin-trapping reaction and transforms the normal EPR responses into a more sensitively luminescent signaling system with the limit of detection improved to 5 nM. Twelve-fold amide groups are also functionalized within the tetrahedron to modify the hydrophilic/lipophilic environment, ensuring the successful application of biological imaging in living cells.

Metal–organic polyhedra (MOPs), discrete molecular architectures constructed through the coordination of metal ions and organic linkers, have attracted considerable attention for their potential for a variety of applications due to their high symmetry, stability, and rich chemical/physical properties.<sup>1–4</sup> These molecules are synthesized by using modular and high-yield metal-directed self-assembled methods, so that the geometric and electronic characteristics embedded within the individual components have collectively allowed the construction of the supramolecular entities in a controllable way.<sup>5–8</sup> The architectures generating well-defined cavities with gated pores provide specific inner environments for selective uptake and binding of guest molecules and catalyzing their reactions.<sup>9,10</sup> In parallel to the impressive development of this field in the past two decades, the research of fluorescent biological imaging has also grown into a mature field.<sup>11,12</sup> In comparison, the science at the interface between the well-confined MOP systems and the detection and imaging techniques by luminescence response in biological cells has received relatively little attention.

Without doubt, the major challenges for the well-confined MOP systems applied to biological imaging detection go beyond achieving molecular recognition, and include the modifying hydrophilic/lipophilic characterization of MOPs, potentially helpful to exhibit biocompatibility and cell permeability.<sup>13</sup> In this case, the neutral molecular systems rather than the ionic metallacycles would benefit the biological applications. As nature has

served as a dominant source of inspiration in the area of supramolecular chemistry, the functionalization with amide groups, the characteristic structural motif of protein, on the metal–organic cages should be a useful attempt to achieve functional metal–organic polyhedra with suitable hydrophilic/lipophilic characterization.<sup>14</sup> By incorporating robust amide-containing tridentate chelating sites into the three arms of a triphenylamine fragment, the often-used energy donor and bright blue emitter,<sup>15,16</sup> we obtained a cerium-based neutral molecular tetrahedron, **1**. This tetrahedron is able to encapsulate 2-phenyl-4,4,5,5-tetra-methylimidazolineyloxyl-3-oxide (PTIO), one of the most stable nitronyl nitroxides known and a specific spin-labeling NO trapper used for detecting NO in biological systems.<sup>17–21</sup> The confinement of the cavity of tetrahedron **1** can force the NO and PTIO species close to each other, prompting the specific spin-trapping reaction and restoring the luminescence of compound **1**. With compound **1**, the biological detection of NO at a limit of 5 nM and the biological imaging of NO in living cells are realized, whereas other reactive nitrogen and oxygen species do not give any detectable luminescence responses.

Ligand H<sub>6</sub>TTS was synthesized from 4,4',4''-nitritotribenzocarbonylhydrazide with salicylaldehyde in methanol solution and characterized by elemental analysis and spectroscopic methods. Diffuse CH<sub>3</sub>OH to a DMF solution of H<sub>6</sub>TTS containing Ce(NO<sub>3</sub>)<sub>3</sub>·6H<sub>2</sub>O generated **1**, in a high yield (65%). Magnetic susceptibility measurements suggested a diamagnetic behavior of the bulk sample from room temperature to 1.8 K, demonstrating the presence of four Ce<sup>IV</sup> ions of **1**. Ce 3d core level XPS spectrum exhibited a distinct band at about 916 eV, which was assignable beside the peaks at around 880–890, 895–910 distinct regions. The unique peak was assigned to 4f<sup>0</sup> orbital transitions,<sup>22,23</sup> which confirmed the presence of oxidation state Ce<sup>IV</sup> in **1**. The bonding of the ligands to the metal ions was also confirmed by the relatively broadened and shifted resonance signals in <sup>1</sup>H NMR spectra. Precisely, the disappearance of the phenolic proton signal at ~11.33 ppm and the significant upfield shift of aromatic protons in the phenol ring suggested the coordination occurred between the deprotonated phenolic groups and the metal ions.<sup>24</sup> The downfield shift from 12.10 to 13.17 ppm and the reduction of the proton portion of the amide signal were indicative of the coordination of amide groups to the metal ions and the partial deprotonation of amide groups during the coordination process.

Received: May 26, 2011

Published: July 12, 2011

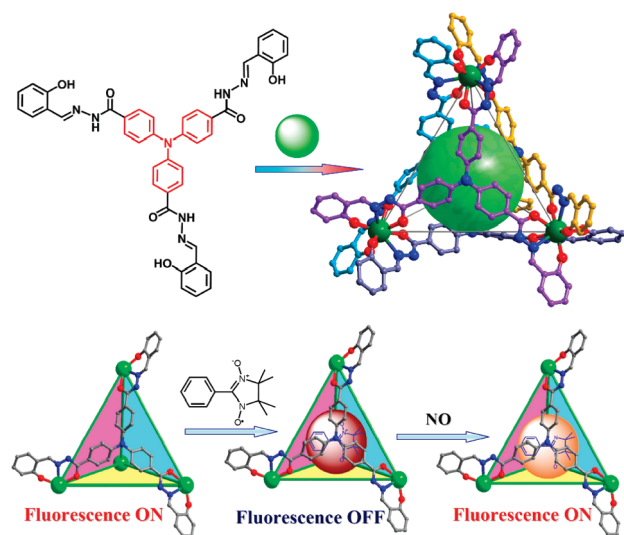


**Figure 1.** Structure of  $H_2TTS$ , constitutive/constructional fragments of the functional tetrahedron **1** showing the sequence of fluorescent variation of the tetrahedron **1** upon the addition of PTIO and NO.

Single-crystal X-ray structural analysis confirmed the formation of a  $Ce_4(H_2TTS)_4$  tetrahedron in a crystallographic  $C_3$  symmetry in the solid state (Figure 1).<sup>25</sup> The tetrahedron comprised four vertical metal centers and four deprotonated  $H_2TTS$  ligands. Each cerium ion was chelated by three tridentate-chelating groups from three different ligands to form a ternate coronary trigonal prism coordination geometry with a pseudo- $C_3$  symmetry. The four pseudo- $C_3$  symmetric planar ligands positioned individually on the four triangle faces of the tetrahedron defined by four metal ions. The  $Ce \cdots Ce$  separation was  $\sim 14.9$  Å, the inner volume of the tetrahedron is about  $360$  Å<sup>3</sup>, and the rhombic window of the tetrahedron had a size of  $6.5 \times 6.5$  Å<sup>2</sup>, potentially allowing ingress and egress of small molecules. The  $Ce-O$  (phenol) and  $Ce-O$  (amide) distances of 2.24, and 2.43 Å, respectively, and the  $Ce-N$  distance of 2.67 Å were in good agreement with the relative compounds,<sup>26,27</sup> with the valences of the two cerium centers calculated as 3.9 and 4.0 for  $Ce(1)$  and  $Ce(2)$ , respectively.<sup>28,29</sup> The  $C-O$  and  $C-N$  distances of 1.26 Å and 1.34 Å, respectively, were intermediate between formal single and double bonds, indicating extensive delocalization over the entire molecular skeleton.<sup>30</sup> The absence of any ionic species in the crystal structure suggested that the tetrahedron **1** was neutral. Referring to the  $^1H$  NMR investigation, all the phenol groups and one-third of the amide groups were deprotonated. The protonated and deprotonated amide groups are expected to build a suitable hydrophilic/lipophilic environment of the cavity.

ESI-MS (negative) spectrum of **1** in DMF/ $CH_3OH$  solution exhibited two intense peaks at  $m/z = 1155.78$  and  $1734.14$  with the isotopic distribution patterns separated by 0.33 and 0.50 Da, respectively. By comparison of the experimental peaks with the simulation results obtained based on natural isotopic abundances, the peaks were assigned to the species  $[Ce_4(H_2TTS)_3-(H_2TTS)]^{3-}$  and  $[Ce_4(H_2TTS)_2(H_2TTS)_2]^{2-}$ , respectively, demonstrating the formation of  $M_4L_4$  species in the solution. Upon the addition of the free radical PTIO, ESI-MS exhibited a new peak at  $m/z \sim 1233.80$  with the isotopic distribution patterns separated by 0.33 Da. This peak is assignable to the host-guest complexation species  $[Ce_4(H_2TTS)_3(H_2TTS) \supset PTIO]^{3-}$ ,

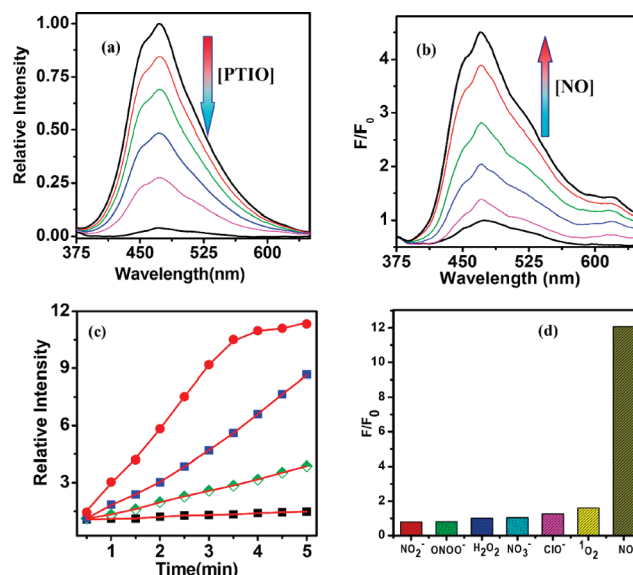


**Figure 2.** Families of the luminescence spectra of (a) **1** ( $15 \mu M$ ) upon addition of the free radical PTIO up to  $0.45$  mM. (b) **1** ( $15 \mu M$ ) and PTIO ( $0.30$  mM) upon addition of NO up to  $0.45$  mM. (c) Time-dependent luminescence variations of **1** ( $15 \mu M$ ) and PTIO ( $0.30$  mM) showing the recovery of luminescence upon the addition of the NO with the concentration  $0.1$ ,  $0.2$ ,  $0.3$ , and  $0.4$  mM (black, green, blue, and red symbols, respectively). (d) Luminescence selectivity of **1** ( $15 \mu M$ ) and PTIO ( $0.3$  mM) treated with various ROS and RNS. NO:  $0.5$  mM;  $H_2O_2$ :  $1.0$  mM;  $OCI^-$ :  $1.0$  mM NaOCl;  $O_2$ :  $1.0$  mM  $H_2O_2$  +  $1.0$  mM NaOCl;  $NO_2^-$ :  $1.0$  mM NaNO<sub>2</sub>;  $NO_3^-$ :  $1.0$  mM NaNO<sub>3</sub>;  $ONOO^-$ :  $1.0$  mM NaONOO. Intensities were recorded at  $470$  nm, with the excitation at  $350$  nm.

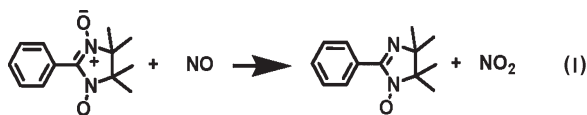
which demonstrates a 1:1 stoichiometric inclusion behavior in solution.

Compound **1** exhibited an absorption band centered at  $395$  nm ( $\log \epsilon = 5.07$ ) assignable to the absorptions endemic to deprotonated phenol groups.<sup>31</sup> When excited at  $350$  nm in DMF, **1** ( $15 \mu M$ ) exhibited an emission band centered on  $470$  nm with a quantum yield of  $0.01$ <sup>32</sup> (Figure 2). Upon the addition of free radical PTIO up to  $0.30$  mM, the luminescence intensity of the solution decreased gradually with  $\sim 90\%$  quenching efficiency and  $EC_{50}$  (the concentration of guest added that half quenched the luminescence) of about  $40 \mu M$ . The Hill-plot<sup>33</sup> of the fluorescence titration curves demonstrated a 1:1 stoichiometric host-guest behavior with an association constant ( $\log K_{ass}$ ) of  $4.78 \pm 0.2$ .

Nitric oxide (NO) is an important mediator for both physiological and pathophysiological processes, and a key player in numerous mammalian functions including vasodilation, immune responses, and neurotransmission.<sup>34</sup> Due to its large diffusivity and high reactivity with other radicals and metal-containing proteins in biological systems, the development of methods capable of detecting NO in biology have been an intriguing challenge for chemists, biologists, and engineers.<sup>35–37</sup> Nitronyl nitroxides are stable radicals and have been extensively applied as NO trappers for the detection of NO in biological systems.<sup>17–21</sup> However this spin-trapping technique is limited by the low sensitivity of the EPR technique and the low resolution of EPR image resolution as well as the large sample size of the EPR detection.<sup>34</sup> Interestingly, introducing NO ( $0.45$  mM) into the mixture containing  $15 \mu M$  **1** and  $0.3$  mM PTIO in DMF/ $H_2O$

(9:1) media at room temperature immediately restored the luminescence of **1** with a 12-fold increase of intensity within 5 min. Since fluorescence illumination and observation has been one of the most rapidly adopted imaging technologies in medicine and biological sciences, this new probing approach would be a useful attempt to transform the spin-trapping responses into a luminescence signaling system.

EPR spectra of the mixture containing **1** (1 mM) and PTIO (30 mM) at room temperature clearly exhibited change in the EPR signal pattern of PTIO from the characteristic five-line pattern with first derivation peak height ratios of 1:2:3:2:1 to a seven-line one with corresponding ratios of 1:1:2:1:2:1:1 upon the addition of 40 mM NO. This result is well consistent with that of PTIO itself without the presence of the tetrahedron and confirms the occurrence of the reaction shown in eq 1 in the solution.<sup>19</sup>



Usually, nitronyl and imino nitroxides are nonspecifically reduced by various biological reductants. To avoid the interference from the redox systems in endothelial cells, nitronyl nitroxides are usually mixed with the effluent from an endothelial cell column.<sup>38</sup> For our probing system, the probing process could not be disturbed by the presence of other reactive species in the EPR measurement, and the luminescence measurement of the mixture containing 15  $\mu\text{M}$  of compound **1** and 0.3 mM of PTIO in DMF/H<sub>2</sub>O (9:1) media upon the addition of reactive species including H<sub>2</sub>O<sub>2</sub>, <sup>1</sup>O<sub>2</sub>, ClO<sup>−</sup>, NO<sub>2</sub><sup>−</sup>, NO<sub>3</sub><sup>−</sup>, and ONOO<sup>−</sup> hardly exhibited obvious luminescence variation.<sup>39</sup> The high selectivity toward nitric oxide over other species is likely due to the special environment provided by the cavities of the polyhedron. That is to say, the encapsulation of spin-trapping agent PTIO within the cavities of the luminescent metal–organic polyhedron provides a new probing method with significantly improved selectivity over the traditional systems.

Importantly, our system is able to respond NO in an apparent pH range from 5.0 to 9.0 (DMF/H<sub>2</sub>O = 7:3), with the fluorescence intensity varying by less than 10%, facilitating the detection of NO in aqueous media at physiological pH. Under optimized conditions, the fluorescence intensity of the probing solution (1.5  $\mu\text{M}$  **1** and 30  $\mu\text{M}$  PTIO) was nearly proportional to the NO concentration, and the purging of 5 nM NO causes about 15% fluorescent enhancement within 5 min at 298 K. The detection limit of 5 nM established is comparable to that of the most sensitive NO sensors reported<sup>40,41</sup> and is quite lower than the practical EPR detection limit (0.1–0.01  $\mu\text{M}$ ).<sup>42</sup> Clearly, the turn-on response manner has sensitivity higher than the traditional spin-trapping platform. Accordingly, the high sensitivity and selectivity coupled with the solubility in aqueous media of the probe made it a superior probe for NO detection by biological imaging.

Another interesting finding is about the kinetic behavior of the probing. Typically, the spin-trapping reaction between PTIO and NO shows a second-order rate kinetic behavior<sup>43</sup> with the constant of  $5.15 \times 10^3 \text{ M}^{-1} \text{ s}^{-1}$ . Our new system exhibited a pseudo-zeroth-order kinetic behavior under saturation conditions, i.e. having quite large NO and PTIO concentration. It seems that the spin-trapping reaction is significantly catalyzed

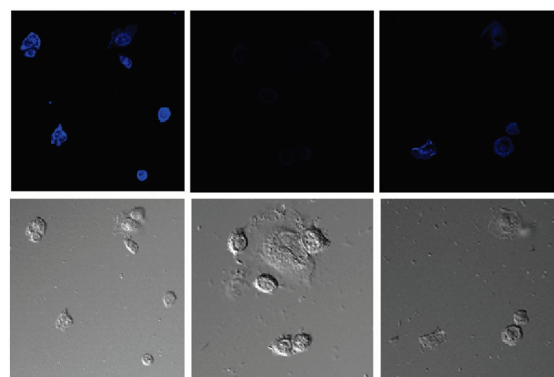


**Figure 3.** Fluorescence imaging of compound **1** (15  $\mu\text{M}$ , suspended in DMF) and PTIO (20  $\mu\text{M}$ , suspended in DMF) induced by sodium nitroprusside (2.0 mM). (Bottom row) Brightfield images of MCF-7 cells shown in top panel. Fluorescence image of MCF-7 cells incubated with compound **1** (top left); incubated with PTIO in top row (middle); further incubated with sodium nitroprusside (top right). Excited at 405 nm.

and typically enzymatic-like, governed by the Michaelis–Menten mechanism,<sup>44</sup> in which substrate binding is a first equilibrium prior to the rate-limiting step of the reaction. As a comparison, addition of PTIO (0.45 mM) to the solution of the free ligand H<sub>6</sub>TTS (60  $\mu\text{M}$ ) or triphenylamine (60  $\mu\text{M}$ ) only caused a less than 15% intensity decrease of the luminescence at 435 and 405 nm, and further addition of NO to the above-mentioned solution did not lead to any obvious fluorescence variation within 60 min. The confinement of the cavity of compound **1** as an analogy of the pocket of an enzyme could accelerate the reaction through proximity effects and increases the local concentration of the substrates.<sup>1,45</sup>

To test its applicability in living system, we investigated **1** in MCF-7 cells using fluorescence microscopy. The cells were incubated with a 15  $\mu\text{M}$  solution of compound **1** (suspended in phosphate-buffered saline [PBS]) for 30 min at room temperature. Then the cells were washed with PBS three times and mounted on a microscope stage. As shown in Figure 3, the cells display blue luminescence after incubation by compound **1**. The cells remained viable throughout the imaging experiments (about 3–4 h). Incubated with 20  $\mu\text{M}$  PTIO, the luminescence of the system was not visible, indicating that PTIO in the cell was fluorescently detected by compound **1**. The solution was further incubated with sodium nitroprusside (2.0 mM) for another 30 min at room temperature; the intense blue fluorescence of cells was resumed. These experiments proved that our system could be used for monitoring intracellular NO, and compound **1** is the first example of metal–organic polyhedra successfully used for biological imaging in living cells. The combination of spin-trapping agents within the cavity of the luminescent metal–organic cages thus represents a more powerful approach to the high-sensitivity luminescent detections than the traditional EPR response methods.

In a summary, this work represents the first example of molecular tetrahedra that enables the application of biological imaging of NO in living cells. The metal–organic tetrahedron **1** can function as an enzyme-like pocket to encapsulate the spin-trapping agent molecule and prompt the spin-trapping reaction with NO occurring in biological systems. In the presence of NO, the quenched luminescence of triphenylamine fragments was



ignited by the spin trapping reaction, which essentially wiped out the luminescence quenchers. The EPR response was substituted by the highly selective and sensitive, rapidly adapted, luminescent imaging technology.

## ■ ASSOCIATED CONTENT

**S Supporting Information.** Crystal data (CIF file), experimental details, and the host–guest properties. This material is available free of charge via the Internet at <http://pubs.acs.org>.

## ■ AUTHOR INFORMATION

### Corresponding Authors

hecheng@dlut.edu.cn, cyduan@dlut.edu.cn

## ■ ACKNOWLEDGMENT

We gratefully acknowledge financial support from the NSFC (20801008 and 21025102).

## ■ REFERENCES

- (1) Yoshizawa, M.; Klosterman, J. K.; Fujita, M. *Angew. Chem., Int. Ed.* **2009**, *48*, 3418–3438.
- (2) Cronin, L. *Angew. Chem., Int. Ed.* **2006**, *45*, 3576–3578.
- (3) Lützen, A. *Angew. Chem., Int. Ed.* **2005**, *44*, 1000–1002.
- (4) Pluth, M. D.; Bergman, R. G.; Raymond, K. N. *Acc. Chem. Res.* **2009**, *42*, 1650–1659.
- (5) Northrop, B. H.; Zheng, Y. R.; Chi, K. W.; Stang, P. J. *Acc. Chem. Res.* **2009**, *42*, 1554–1563.
- (6) Tranchemontagne, D. J.; Ni, Z.; O’Keeffe, M.; Yaghi, O. M. *Angew. Chem., Int. Ed.* **2008**, *47*, 5137–5147.
- (7) Hamilton, T. D.; Papaefstathiou, G. S.; Friscic, T.; Bucar, D. K.; MacGillivray, L. R. *J. Am. Chem. Soc.* **2008**, *130*, 14366–14367.
- (8) Dinolfo, P. H.; Hupp, J. T. *Chem. Mater.* **2001**, *13*, 3113–3125.
- (9) Fox, O. D.; Cookson, J.; Wilkinson, E. J. S.; Drew, M. G. B.; MacLean, E. J.; Teat, S. J.; Beer, P. D. *J. Am. Chem. Soc.* **2006**, *128*, 6990–7002.
- (10) Yoshizawa, M.; Tamura, M.; Fujita, M. *Science* **2006**, *312*, 251–254.
- (11) Kobayashi, H.; Ogawa, M.; Alford, R.; Choyke, P. L.; Urano, Y. *Chem. Rev.* **2010**, *110*, 2620–2640.
- (12) Kikuchi, K. *Chem. Soc. Rev.* **2010**, *39*, 2048–2053.
- (13) Sakai, N.; Matile, S. *Angew. Chem., Int. Ed.* **2008**, *47*, 9603–9607.
- (14) Ferrand, Y.; Crump, M. P.; Davis, A. P. *Science* **2007**, *318*, 619–622.
- (15) Ning, Z. J.; Tian, H. *Chem. Commun.* **2009**, 5483–5495.
- (16) Hagfeldt, A.; Boschloo, G.; Sun, L. C.; Kloo, L.; Pettersson, H. *Chem. Rev.* **2010**, *110*, 6595–6663.
- (17) Osiecki, J. H.; Ullman, E. F. *J. Am. Chem. Soc.* **1968**, *90*, 1078–1079.
- (18) Ullman, E. F.; Call, L.; Osiecki, J. H. *J. Org. Chem.* **1970**, *35*, 3623–3631.
- (19) Nadeau, J. S.; Boock, D. G. B. *Anal. Chem.* **1977**, *49*, 1672–1676.
- (20) Yoshida, M.; Akaike, T.; Goto, S.; Takahashi, W.; Inadome, A.; Yono, M.; Seshita, H.; Maeda, H.; Ueda, S. *Lifesciences* **1998**, *62*, 203–211.
- (21) Haruyama, T.; Shiino, S.; Yanagida, Y.; Kobatake, E.; Aizawa, M. *Biosens. Bioelectron.* **1998**, *13*, 763–769.
- (22) Larachi, F.; Pierre, J.; Adnot, A.; Bernis, A. *Appl. Surf. Sci.* **2002**, *195*, 236–250.
- (23) Datta, P.; Majewski, P.; Aldinger, F. *Mater. Charact.* **2009**, *60*, 138–143.
- (24) Li, Y.; Yang, Z. Y.; Wang, M. F. *J. Fluoresc.* **2010**, *20*, 891–905.
- (25) Crystal data: Ce-TTS  $C_{178}H_{148}Ce_4N_{30}O_{31}$  [ $Ce_4(C_{42}H_{29}N_7O_6)_4 \cdot 2C_3H_7NO \cdot 4CH_3OH \cdot H_2O$ ],  $M = 3763.74$ , Hexagonal, space group  $R\bar{3}c$ , black block,  $a = 30.93(1)$  Å,  $c = 86.90(6)$  Å,  $V = 71982(65)$  Å<sup>3</sup>,  $Z = 12$ ,  $D_c = 1.042$  g cm<sup>-3</sup>,  $\mu(Mo K\alpha) = 0.802$  mm<sup>-1</sup>,  $T = 180(2)$  K. 14083 unique reflections [ $R_{int} = 0.1135$ ]. Final  $R_1$  [with  $I > 2\sigma(I)$ ] = 0.0692,  $wR_2$  (all data) = 0.2031. CCDC number 798012.
- (26) Terzis, A.; Mentzafos, D.; Riahi, H. A. T. *Inorg. Chim. Acta* **1984**, *84*, 187–193.
- (27) Yang, S. P.; Han, L. J.; Wang, D. Q.; Wang, B. *Acta Crystallogr., Sect. E* **2007**, *63*, m2777–m2778.
- (28) Brese, N. E.; O’Keeffe, M. *Acta Crystallogr., Sect. B* **1991**, *47*, 192–197.
- (29) Brown, I. D.; Altermatt, D. *Acta Crystallogr., Sect. B* **1985**, *41*, 244–247.
- (30) Stadler, A. M.; Harrowfield, J. *Inorg. Chim. Acta* **2009**, *362*, 4298–4314.
- (31) Biernacka, I. K.; Bartecki, A.; Kurzak, K. *Polyhedron* **2003**, *22*, 997–100.
- (32) Juris, A.; Balzani, V.; Barigelletti, F.; Campagna, S.; Belser, P.; von Zelewsky, A. *Coord. Chem. Rev.* **1988**, *84*, 85–277.
- (33) Connors, K. A. *Binding Constants*; John Wiley: New York, 1987.
- (34) Nagano, T.; Yoshimura, T. *Chem. Rev.* **2002**, *102*, 1235–1269.
- (35) Kim, J. H.; Heller, D. A.; Jin, H.; Barone, P. W.; Song, C.; Zhang, J.; Trudel, L. J.; Wogan, G. N.; Tannenbaum, S. R.; Strano, M. S. *Nature Chem.* **2009**, *1*, 473–481.
- (36) Yang, Y. J.; Seidlits, S. K.; Adams, M. M.; Lynch, V. M.; Schmidt, C. E.; Anslyn, E. V.; Shear, J. B. *J. Am. Chem. Soc.* **2010**, *132*, 13114–13116.
- (37) Sasaki, E.; Kojima, H.; Nishimatsu, H.; Urano, Y.; Kikuchi, K.; Hirata, Y.; Nagano, T. *J. Am. Chem. Soc.* **2005**, *127*, 3684–3658.
- (38) Haseloff, R. F.; Zollner, S.; Kirilyuk, I. A.; Grigorev, I. A.; Reszka, R.; Bernhardt, R.; Mertsch, K.; Roloff, B.; Blasig, I. E. *Free Radical Res.* **1997**, *26*, 7–17.
- (39) Kundu, K.; Knight, S. F.; Willett, N.; Lee, S.; Taylor, W. R.; Murthy, N. *Angew. Chem., Int. Ed.* **2009**, *48*, 299–303.
- (40) Kojima, H.; Urano, Y.; Kikuchi, K.; Higuchi, T.; Hirata, Y.; Nagano, T. *Angew. Chem., Int. Ed.* **1999**, *38*, 3209–3212.
- (41) Zheng, H.; Shang, G. Q.; Yang, S. Y.; Gao, X.; Xu, J. G. *Org. Lett.* **2008**, *10*, 2357–2360.
- (42) Davies, M. J.; Timmins, G. S. *Biomedical Application of Spectroscopy*; Clark, R. J., Hester, R. E., Eds.; John Wiley & Sons: New York, 1996; p 217.
- (43) Akaike, T.; Yoshida, M.; Miyamoto, Y.; Sato, K.; Kohno, M.; Sasamoto, K.; Miyazaki, K.; Ueda, S.; Maeda, H. *Biochemistry* **1993**, *32*, 827–832.
- (44) McKee, T.; McKee, J. R. *Biochemistry: The Molecular Basis of Life*, 3rd ed.; McGraw-Hill: New York, 2003.
- (45) Fiedler, D.; van Halbeek, H.; Bergman, R. G.; Raymond, K. N. *J. Am. Chem. Soc.* **2006**, *128*, 10240–10252.